Respiratory Research

RESEARCH

Open Access

Cromolyn sodium reduces LPS-induced pulmonary fibrosis by inhibiting the EMT process enhanced by MC-derived IL-13

Cheng Tan[1†], Hang Zhou[2†], Qiangfei Xiong[2], Xian Xian[2], Qiyuan Liu[2], Zexin Zhang[2], Jingjing Xu[1*] and Hao Yao[2*]

Abstract

Background Sepsis is a systemic inflammatory response caused by infection. When this inflammatory response spreads to the lungs, it can lead to acute lung injury (ALI) or more severe acute respiratory distress syndrome (ARDS). Pulmonary fibrosis is a potential complication of these conditions, and the early occurrence of pulmonary fibrosis is associated with a higher mortality rate. The underlying mechanism of ARDS-related pulmonary fibrosis remains unclear.

Methods To evaluate the role of mast cell in sepsis-induced pulmonary fibrosis and elucidate its molecular mechanism. We investigated the level of mast cell and epithelial-mesenchymal transition(EMT) in LPS-induced mouse model and cellular model. We also explored the influence of cromolyn sodium and mast cell knockout on pulmonary fibrosis. Additionally, we explored the effect of MC-derived IL-13 on the EMT and illustrated the relationship between mast cell and pulmonary fibrosis.

Results Mast cell was up-regulated in the lung tissues of the pulmonary fibrotic mouse model compared to control groups. Cromolyn sodium and mast cell knockout decreased the expression of EMT-related protein and IL-13, alleviated the symptoms of pulmonary fibrosis in vivo and in vitro. The PI3K/AKT/mTOR signaling was activated in fibrotic lung tissue, whereas Cromolyn sodium and mast cell knockout inhibited this pathway.

Conclusion The expression level of mast cell is increased in fibrotic lungs. Cromolyn sodium intervention and mast cell knockout alleviate the symptoms of pulmonary fibrosis probably via the PI3K/AKT/mTOR signaling pathway. Therefore, mast cell inhibition is a potential therapeutic target for sepsis-induced pulmonary fibrosis.

Keywords LPS, Pulmonary fibrosis, Mast cell, IL-13, Cromolyn sodium, Sepsis

Introduction

Acute lung injury (ALI) is often induced by pneumonia, pulmonary contusion, alveolar hemorrhage, and sepsis, and in most patients, the condition further deteriorates into acute respiratory distress syndrome (ARDS), which becomes an important cause of death due to respiratory failure [1]. Pathologically, the main features of ALI/ARDS include diffuse alveolar injury and increased alveolar and capillary permeability. As the disease progresses, the alveolar structure may be severely damaged, eventually leading to pulmonary fibrosis (PF) [2–4]. Despite the availability of symptomatic supportive

†Cheng Tan and Hang Zhou have contributed equally to this work.

*Correspondence:
Jingjing Xu
jingjing6104@126.com
Hao Yao
yaohao@njmu.edu.cn
[1] Department of Anesthesiology, The Affiliated Wuxi People's Hospital of Nanjing Medical University, Wuxi People's Hospital, Wuxi Medical Center, Wuxi 214002, Jiangsu Province, China
[2] Department of Anesthesiology, The Second Affiliated Hospital of Nanjing Medical University, Nanjing Medical University, Nanjing 210011, Jiangsu Province, China

clinical treatments, there is still a lack of effective means to slow or reverse the process of fibrosis [5]. The limited understanding of ALI pathogenesis at the molecular level, coupled with the inadequacy of existing therapeutic strategies, has resulted in a high mortality rate in patients with ALI [6]. Therefore, an in-depth exploration of the mechanisms underlying the onset and development of ALI-induced PF at the molecular level is of utmost clinical importance to improve the therapeutic outcome of ALI/ARDS.

Pulmonary fibrosis is not only a pathological process that evolves after lung tissue damage but also the end of many lung diseases. It is characterized by excessive proliferation of fibroblasts and abnormal deposition of extracellular matrix (ECM), which leads to decreased lung compliance, progressive dyspnea, and ultimately respiratory failure. Studies have shown that damage to type II alveolar epithelial cells, interactions between alveolar epithelial cells and fibroblasts, and epithelial–mesenchymal transition (EMT) play critical roles in the pathogenesis of PF [7]. Epithelial-derived fibroblasts account for approximately one-third of pulmonary fibrosis cases. Current theories propose that myofibroblasts transformed from epithelial cells by EMT exhibit abnormal proliferative activity and excessive ECM-producing capacity, which drives the developmental process of PF [8–10]. EMT is active in PF and is a critical step in the pathogenesis of pulmonary fibrosis. EMT is characterized by the loss of epithelial markers, reorganization of the cytoskeleton, and acquisition of mesenchymal markers along with the transition to EMT markers, including epithelial markers such as E-cadherin and mesenchymal markers such as vimentin, N-cadherin, and α-smooth muscle actin (α-SMA).

Mast cells are a class of multifunctional cells of the innate immune system and are widely distributed in various tissues in the body, especially in the skin, intestines and respiratory tract, where they play important roles in maintaining the stability of the tissue microenvironment, participating in immune surveillance, regulating inflammatory responses, and promoting wound healing [11]. Mast cells are abundant in healthy airways and lung parenchyma but are increased in areas of alveolar fibrosis in patients with pulmonary fibrosis caused by a number of different etiologies, including idiopathic pulmonary fibrosis (IPF) and connective tissue-associated pulmonary fibrosis, but their specific role in pulmonary fibrosis remains unknown. Lipopolysaccharides (LPS) can bind to the TLR4 receptor on the surface of mast cells and promote their release of IL-13, but whether LPS plays a beneficial or detrimental role in sepsis-associated pulmonary fibrosis remains unknown [12].

Interleukin-13 (IL-13) is a proinflammatory cytokine produced by cells such as type 2 helper T cells (Th2) [13]. Numerous studies have shown that IL-13 is an important profibrotic factor, and increases in IL-13 have been observed in fibrotic lungs in both human and animal models and have been shown to activate different immune cells, including alveolar macrophages, epithelial cells, and fibroblasts [14, 15]. Among other factors, IL-13 can lead to impaired differentiation of alveolar epithelial cells and promote EMT, which in turn leads to the development of pulmonary fibrosis. However, the specific signaling pathway by which IL-13 promotes EMT remains unknown [16, 17]. The PI3K/AKT signaling pathway is involved in a variety of biological processes, including the cell cycle, apoptosis, angiogenesis, and glucose metabolism [18]. The PI3K/AKT pathway is indispensable for cell proliferation and apoptosis and plays an important role in the onset and progression of pulmonary fibrosis. PI3K/AKT can directly activate the mTOR signaling pathway, leading to downstream signaling cascades that affect cell proliferation, growth, autophagy, and metabolism. In pulmonary fibrosis, damaged alveolar epithelial cells trigger diverse inflammatory responses, repair mechanisms, and signaling pathways, including the PI3K/AKT/mTOR pathway. Activation of these responses and pathways leads to the release of profibrotic mediators, which in turn disrupts the homeostasis between pro-fibrotic and anti-fibrotic mediators, a process that also involves epithelial–mesenchymal transition [19–21]. It has been shown that inhibition of the PI3K/AKT/mTOR pathway suppresses EMT, and the use of AKT inhibitors reverses EMT to a certain extent. These findings reveal that the PI3K/AKT/mTOR pathway plays a crucial role in the EMT process in lung fibrosis [22–24].

In this study, we measured mast cell and IL-13 levels in an animal model of LPS-induced pulmonary fibrosis and evaluated the effects of mast cell inhibition and knockdown on mast cell-derived IL-13 and pulmonary fibrosis and the potential underlying mechanisms through in vivo and in vitro experiments.

Materials and methods

Animals and ethical statement

Male C57BL/6 wild-type mice (aged 6–8 weeks, 20–25 g) were obtained from the Experimental Animal Center of Nanjing Medical University. Male C57BL/6-Kit^{W-sh}/Kit^{W-sh} (kit^{W-sh}) mice were generated in our laboratory, and colonies of these mice were maintained for studies. All the mice were housed in a temperature-controlled room with a 12 h light/12 h dark cycle and sufficient food and water. This study was approved by the Institutional

Animal Care and Use Committee (IACUC) of Nanjing Medical University (No. 2207016).

Murine model of LPS-induced pulmonary fibrosis and treatment

Mice were randomly divided into four groups: the control group (Con group), the Cromolyn sodium group (Cro group), the LPS group, and the LPS + Cro group. To induce pulmonary fibrosis in mice, continuous intraperitoneal injection of *E. coli* LPS serotype 0111: B4 (Sigma, St. Louis, MO) was administered. Mice received intraperitoneal injections of LPS (5 mg/kg) or an equal volume of PBS for 5 consecutive days. For treatment, the mice received intraperitoneal injections of Cro (50 mg/kg) (Sigma, St. Louis, MO) or an equal volume of PBS for 5 consecutive days starting 30 min before LPS injection. Mice in each group were randomly sacrificed on days 0, 7, 14, and 28 after LPS treatment. Lung tissues were rapidly removed, the left lung portion was used for lung histology analysis, and the right lung tissue was rapidly frozen in liquid nitrogen and stored at −80 °C for analysis of relevant indexes.

Histopathology and immunohistochemistry

The right lung tissues were fixed in 4% paraformaldehyde (PFA) for 48 h, embedded in paraffin and cut into 4-μm thick sections. Tissue sections were stained with hematoxylin and eosin (HE) according to the manufacturer's instructions to assess histopathological changes. Lung injury was scored by an experienced pathologist who was blinded to the purpose of the study. Fibrotic areas in the lung sections were assessed using Masson trichrome staining (Sevier, China). Lung fibrosis was scored by an experienced pathologist who was blinded to the purpose of the study, as previously described by Ashcroft et al.

Immunohistochemical staining was used to assess the expression of tryptase, E-cadherin, and vimentin. Briefly, paraffin Sects. (4 μm) of lung tissues were incubated with rabbit antibodies against tryptase (dilution ratio 1:200, Abcam) or E-cadherin and vimentin (dilution ratio 1:200, Proteintech) overnight at 4 °C, followed by incubation with goat anti-rabbit or anti-mouse IgG (Sevier, Wuhan, China) at room temperature for 1 h. Thereafter, the sections were stained with DAB solution (Sevier, China), and the nuclei were stained with hematoxylin. Photographs of the sections were taken using a Leica Qwin System light microscope (Leica, Germany).

Determination of hydroxyproline content

A hydroxyproline colorimetric analysis kit (E-BC-K062-M. Elabscience, China) was utilized to assess the total lung collagen content according to the manufacturer's instructions.

Cell culture and processing

The mouse lung epithelial cell line MLE-12 and mast cell line P815 were obtained from Sevier (Wuhan, China). These cell lines were characterized by short tandem repeat (STR) analysis and tested for mycoplasma contamination. The cells were incubated in DMEM (Gibco, USA) supplemented with 10% fetal bovine serum (Gibco, USA) and 1% penicillin/streptomycin in a humidified environment at 37 °C and 5% CO2. MLE-12 cells (1–1.5 × 105 cells/well) were wall-plated for 24 h in 6-well plates. After pretreatment with Cro (10 μg/ml) in fresh starvation medium for 30 min, MLE-12 and P815 cells were exposed to PBS or LPS (1 μg/mL) and incubated for 24 h at 37 °C. In some experiments, IL-13 siRNA (10 nM) was transfected into P815 cells.

Coculture of P815 and MLE-12 cells

MLE-12 cells (1–1.5 × 105 cells/well) were placed in the 6-well basal chamber of the Transwell system, and P815 cells were placed in the top chamber. After LPS treatment, with or without Cro pretreatment, MLE-12 cells were cocultured with P815 cells in the coculture system for 24 h, after which MLE-12 cells were isolated for analysis.

In vitro IL-13 siRNA transfection

To inhibit IL-13 expression, siRNAs targeting mouse IL-13 mRNA were designed and purchased from Punuo En Biotechnology (Nanjing, China). The best interfering effect of mouse IL-13 siRNA was selected from three mouse IL-13 siRNAs by quantitative real-time polymerase chain reaction (qRT–PCR) and Western blot analysis. siRNA. P815 cells were transfected with IL-13 siRNA (10 nM) for 48 h using the transfection reagent Lipofectamine 3000 (Vazyme, China). The transfected cells were placed in culture medium for subsequent experiments. The sequences of the mouse IL-13 siRNAs used were 5′-UCUCCCAUAA GGGACC CAUTT-3′ (forward) and 5′-AUGGGGUCCCU UAU GGGGAGATT-3′ (reverse).

ELISA kit

IL-13 levels in cell supernatants were determined using a mouse IL-13 ELISA kit (E-EL-M0727. Elabscience, China) according to the manufacturer's instructions.

Immunoblotting assay (Western blot)

Total proteins were extracted from lung tissues and cells with RIPA lysis buffer containing protease inhibitors (Biyun Tian, China). The protein concentration was determined using the BCA method (Thermo Fisher

Scientific, USA), and the proteins were mixed with the upsampling buffer. Each well was loaded with an equal amount of protein sample (~ 50 μg), and some wells were loaded with a pre-stained protein marker (Vazyme). After electrophoresis (80 V for 30 min and 120 V for 60 min), the proteins were transferred to a PVDF membrane (EMD Millipore). The membranes were labeled with primary antibodies against α-SMA (Proteintech), COLA1 (Proteintech), E-cadherin (Proteintech), Vimentin (Proteintech), IL-13 (Proteintech), Tryptase (Abcam), PI3K (Cell Signaling Technology), P-PI3K (Cell Signaling Technology), AKT (Proteintech), P-AKT (Proteintech), mTOR (Proteintech), P-mTOR (Proteintech), Tubulin (Proteintech) and GAPDH (Proteintech) and incubated overnight at 4 °C. After three washes, the membranes were incubated for 2 h at room temperature with horseradish peroxidase (HRP)-conjugated secondary antibodies at a dilution of 1:5000 and color developed using ECL Prime Western Blot detection reagent (Millipore). The membranes were visualized and imaged using a bioimaging system (Bio-Rad, USA). The experiment was repeated three times.

Real-time quantitative polymerase chain reaction (RT–qPCR)

Total RNA was extracted using Freezol reagent (Vazyme, China) according to the manufacturer's instructions. Then, RNA was reverse transcribed to cDNA using a reverse transcription kit (Vazyme, China). Real-time quantitative polymerase chain reaction (RT–qPCR) was performed using SYBR Green (Vazyme, China) on a LightCycler® 384 system (Roche Diagnostics International) for real-time quantitative PCR. Relative gene expression (fold change) was analyzed using the 2-ΔΔCt method. The mouse-specific primers used were as follows:

IL-13 mus (forward), 5' ATTGCATGGGCCTCTGTA ACC 3'.

IL-13 mus (reverse), 5' CCCAGCAAAGTCTGATGT GA 3'.

Tryptase mus (forward), 5' GCCAATGACACCTAC TGGATG 3'.

Tryptase mus (reverse), 5' GAGCTGTACTCTGAC CTTGTTG 3'.

E-cadherin mus (forward), 5' GCTGGACCGAGAGAG TTACC 3'.

E-cadherin mus (reverse), 5' AGGCACTTGACCCTG ATACG 3'.

Vimentin mus (forward), 5' GGAAAGTGGAATCCT TGCAG 3'.

Vimentin mus (reverse), 5' AGCCACGCTTTCATA CTGCT 3'.

GAPDH mus (forward), 5' ATGGCATGGGCTTAC ACCACC 3'.

GAPDH mus (reverse), 5' GAGGCCAATTTTGTC TCCACA 3'.

Immunofluorescence (IF)

Immunofluorescence staining was used to assess the expression levels of E-cadherin and Vimentin. MLE-12 cells were fixed with 4% PFA for 15 min and washed with phosphate buffer solution (PBS). Then, the samples were blocked with 5% BSA (5% bovine serum albumin in PBS) (Solarbio, China) for 30 min. The cells were then incubated with antibodies against E-cadherin (Proteintech) and vimentin (Proteintech) overnight at 4 °C. The cells were washed with PBS for 5 min three times to remove unbound antibodies and then incubated with Alexa Fluor 488-labeled goat anti-rabbit and Cy3-labeled goat anti-mouse secondary antibodies (1:500. Beyotime, China) for 1 h at room temperature. After washing with PBS, the nuclei were labeled with DAPI (Southernbiotech, USA). Fluorescence images of the stained cells were then acquired using a laser scanning confocal microscope (Leica TCS SP8, Leica, Germany).

Statistical analysis

The experimental data are presented as the means ± standard deviations (SDs) and were analyzed using GraphPad Prism 9 (GraphPad Software, USA). A normality test was first performed using D'Agostino & Pearson analysis before analysis. Comparisons between two groups were made using Student's t test. Comparisons among the four groups were analyzed by one-way or two-way analysis of variance (ANOVA), and Tukey's multiple comparisons were selected for the posttest. p values were considered to indicate statistical significance at $^{*}p < 0.05$, $^{***}p < 0.01$, and $^{***}p < 0.001$.

Results

LPS-induced post-inflammatory lung fibrosis and EMT in mice

In clinical practice, sepsis is recognized as the leading cause of ALI and ARDS. LPS is a key trigger in the pathogenesis of sepsis. Numerous studies have been conducted using LPS to model acute lung injury in animals and have shown that typical fibrotic lesions gradually appear in the lung tissues of animals as the disease progresses [25, 26]. Based on this understanding, we adopted the method described by Chandra and successfully constructed an experimental model of LPS-induced lung fibrosis in mice after ALI [27] (Fig. 1A). Histopathological HE staining of lung tissue revealed that the control group presented normal lung tissue morphology. On the 7th day of the experimental group, congestion and

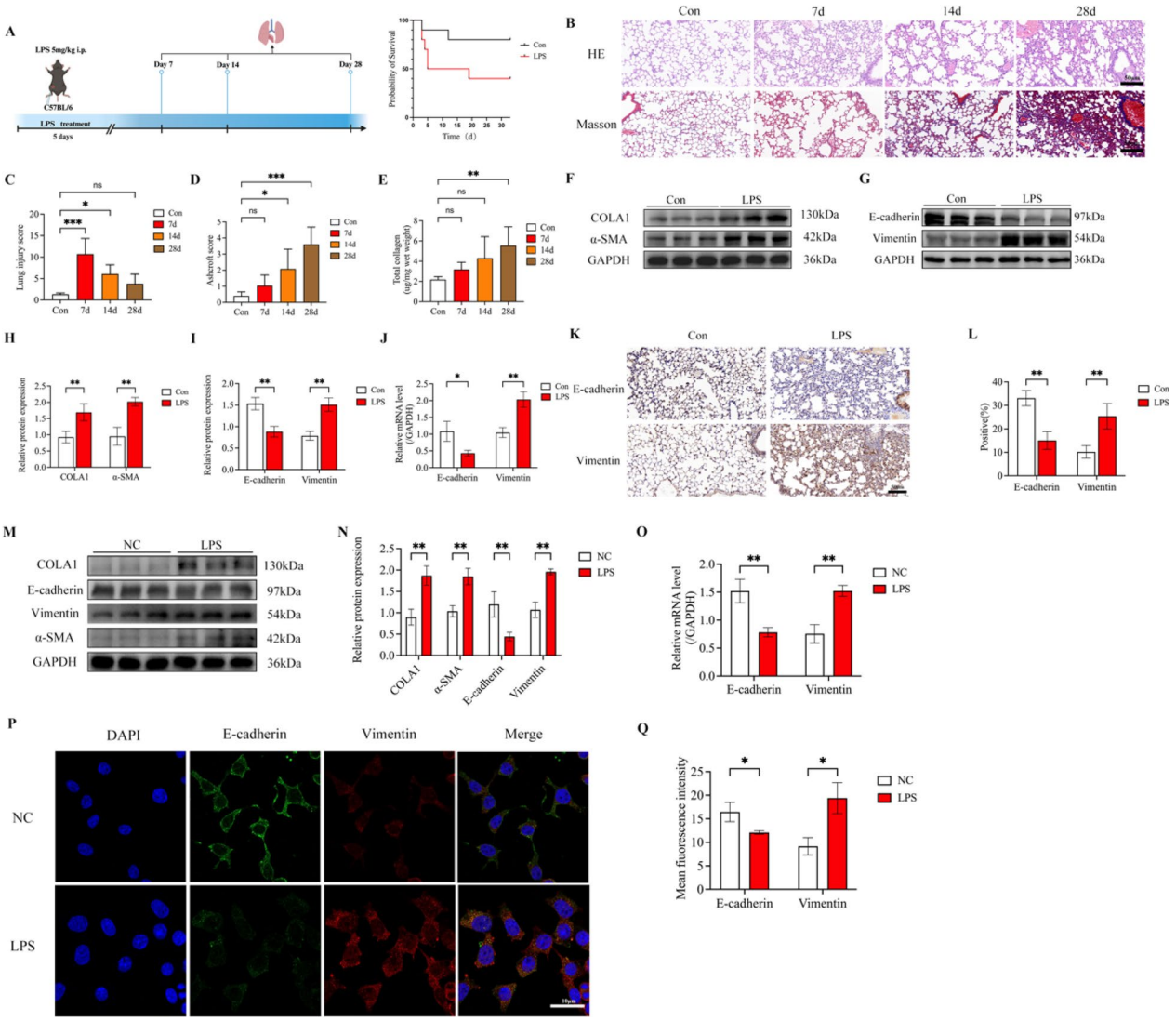

Fig. 1 LPS-induced EMT and post-inflammatory lung fibrosis in mouse lungs. **A** Schematic diagram of the animal model and survival rate. **B** Representative HE and Masson staining results after LPS injection at different times; scale bar: 50 μm. **C**, **D** Lung injury scores and Ashcroft scores according to the HE and Masson staining results, n = 5. **E** Determination of hydroxyproline levels in mouse lung tissues, n = 5. **F**, **H** Representative protein bands of interstitial lung indicators and statistical analysis, n = 3. **G**, **I** Representative EMT protein bands and statistical analysis, n = 3. **J** Expression level analysis of EMT-associated protein mRNA, n = 6. **K**, **L** Immunohistochemistry and positivity rate analysis of EMT-associated proteins; scale bar: 50 μm, n = 5. **M**, **N** Representative bands and statistical analysis of mesenchymal and EMT indexes in MLE-12 cells induced by LPS; n = 3. **O** Expression level analysis of EMT-associated protein mRNA in MLE-12 cells, n = 6. **P**, **Q** Statistical analysis of representative fields of view and fluorescence intensity of immunofluorescence of EMT-related proteins in MLE-12 cells; scale bar: 10 μm, n = 3.*p < 0.05, ***p < 0.01, ***p < 0.001

edema in some lung regions were visible, inflammatory cells in the alveolar spaces increased significantly, local alveoli atrophied, and hemorrhage was observed in some alveolar lumens. On the 14th and 28th days, inflammation in the lung tissue of the mice in the model group was gradually reduced, but the morphology of the lung tissue was significantly altered. The number of normal alveolar structures gradually decreased, consistent with the lung injury score (Fig. 1B, C). Masson staining revealed a small amount of blue staining of the lung tissue in the control group, which is an extracellular matrix collagen component of normal lung tissue. Bluish staining was observed in the mice in the model group on the 7th day, suggesting that collagen deposition occurred in the lungs of the mice at the early stage of inflammation. With increasing time, the amount of bluish fibrous tissue deposited in the lung tissues of the mice on the 14th and 28th days increased gradually, suggesting that the fibroproliferative

response of the lungs of the mice gradually strengthened and that fibrosis reached its highest degree on the 28th day. The Ashcroft score was also in agreement with the staining results (Fig. 1B, D). After that, we measured the levels of the interstitial indicators hydroxyproline, collagen 1, and α-SMA. The ELISA and WB results showed that the levels of collagen 1 and α-SMA in the interstitial of the lung tissues of the model group were significantly increased on day 28 (Fig. 1E, F, H), which is a typical feature of lung fibrosis. To verify whether LPS promotes the development of pulmonary fibrosis by inducing EMT, we measured the expression of E-cadherin, a classical epithelial indicator of EMT, and vimentin, a classical mesenchymal indicator of EMT. The results of both WB and PCR showed that at 28 days of modeling, the protein and mRNA levels of E-cadherin were significantly decreased, whereas the opposite trend was observed for Vimentin, which showed an increasing trend (Fig. 1G). showed an increasing trend (Fig. 1G, I, J). The immunohistochemical results also further verified the occurrence of EMT (Fig. 1K, L).

In addition to the animal model, we selected the MLE-12 mouse alveolar epithelial cell line for in vitro validation by Xiao's method [28]. The EMT model was induced by 1 μg/ml LPS, and the results of WB and PCR showed that the levels of epithelial markers in MLE-12 cells were significantly decreased, while the levels of the mesenchymal indicators collagen 1, α-SMA, and vimentin were significantly increased, and EMT occurred (Fig. 1M–O). This finding was further verified by the immunofluorescence results (Fig. 1P, Q).

Cromolyn sodium inhibits LPS-induced mast cell activation and IL-13 expression

Cromolyn sodium can stabilize the cell membrane of mast cells and inhibit the release of intracellular particulate matter to play an anti-allergic role and inhibit the release of inflammatory cells, of which IL-13 is an important effector that is closely related to EMT and pulmonary fibrosis. Therefore, in further experiments, to investigate the effect of Cromolyn sodium on mice with pulmonary fibrosis, we analyzed the levels of lung mast cells and the expression of IL-13 in mice before and after modeling. First, the results of immunohistochemistry, WB and PCR showed that tryptase levels were significantly elevated in the lung tissues of mice after modeling, and at the same time, the levels of IL-13 were also significantly increased (Fig. 2A–E). After that, according to Roviezzo's experimental method, we intervened by intraperitoneal injection of 50 mg/kg Cromolyn sodium 30 min before each intraperitoneal injection of LPS [29]. After treatment with Cromolyn sodium, the levels of tryptase and IL-13 were reversed in the lung tissues of the mice, indicating that Cromolyn sodium inhibited LPS-induced mast cell activation and IL-13 expression in vivo (Fig. 2F–J).

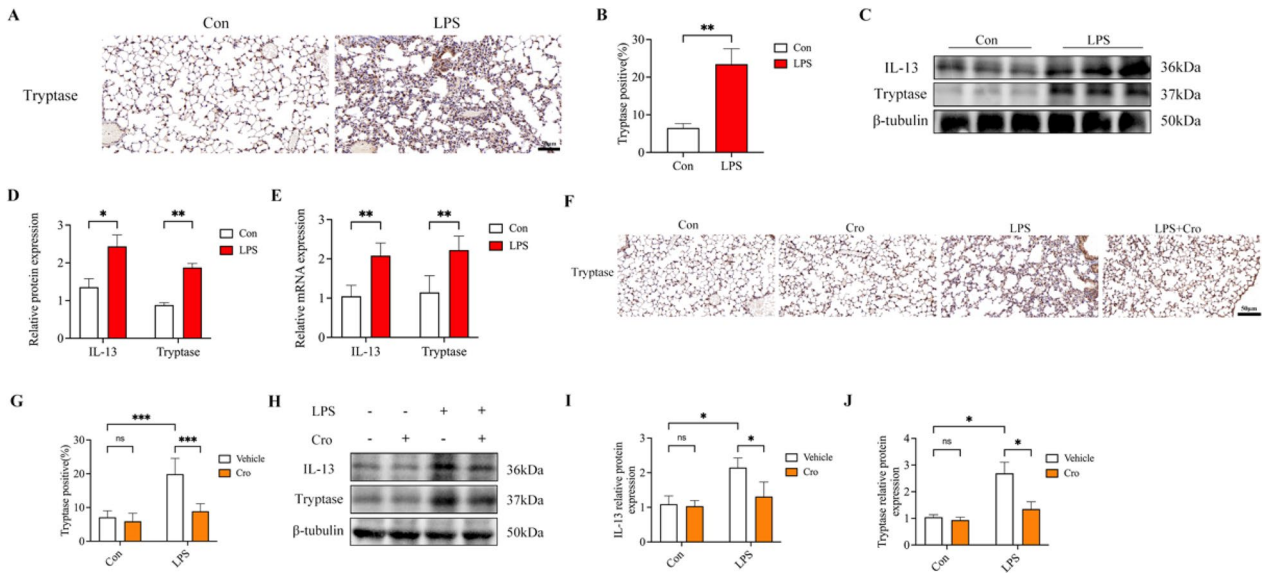

Fig. 2 Cromolyn sodium inhibits LPS-induced mast cell activation and IL-13 expression. **A**, **B** Representative results of Tryptase immunohistochemistry and analysis of the percentage of positive cells; scale bar: 50 μm, n = 5. **C**, **D** Representative protein bands of Tryptase and IL-13 and statistical analysis, n = 3. **E** Expression level analysis of tryptase and IL-13 mRNA, n = 6. **F**, **G** Representative results of tryptase immunohistochemistry and analysis of the percentage of positive cells after Cromolyn sodium intervention; scale bar: 50 μm, n = 5. **H**–**J** Representative protein bands of Tryptase and IL-13 after Cromolyn sodium intervention and statistical analysis, n = 3. *p < 0.05, **p < 0.01, ***p < 0.001

Cromolyn sodium alleviates pulmonary fibrosis by inhibiting EMT

Previous experiments have demonstrated that LPS can promote the development of pulmonary fibrosis by inducing EMT both in vivo and in vitro. To verify whether Cromolyn sodium could alleviate pulmonary fibrosis by inhibiting EMT, we conducted the following experiments. The Masson staining results were consistent with the previous results, and the control group and the Cro group exhibited normal lung tissues, with only a small amount of interstitial collagen. However, the LPS model group exhibited a large amount of collagen deposition, and obvious pulmonary fibrosis occurred. In contrast, after treatment with Cromolyn sodium, collagen deposition in the lung tissue of mice was significantly reduced, and the morphology and scores of the lung tissue were significantly improved (Fig. 3A, B). The ELISA and WB results showed that the levels of the indicators of the lung interstitial, collagen 1, and α-SMA, were significantly increased, which further verified the occurrence of lung fibrosis (Fig. 3C–F). Moreover, treatment with Cromolyn sodium also reversed the changes in the expression of E-cadherin and Vimentin and inhibited the occurrence of EMT (Fig. 3G–N). Taken together, the results showed that Cromolyn sodium suppressed the LPS-induced EMT process in lung tissue and ameliorated pulmonary fibrosis after acute lung injury in mice.

Cromolyn sodium inhibits EMT and attenuates pulmonary fibrosis by reducing mast cell-derived IL-13 release (in vivo)

To determine whether sepsis-induced pulmonary fibrosis is truly related to mast cells and whether IL-13 is of mast cell origin, C57BL/6-Kit^{W-sh}/Kit^{W-sh} (kitW-sh) mast cell knockout mice were used in this study, and the degree of pulmonary fibrosis, the level of IL-13 and the related indexes of EMT in the knockout mice after modeling were evaluated. As shown in Fig. 4A, B, after modeling, Masson staining revealed that the degree of lung fibrosis was significantly reduced in Kit^{W-sh} mice and was similar to that after Cromolyn sodium intervention, a finding verified by the Ashcroft score. In addition, the levels of hydroxyproline, collagen 1, and α-SMA in the intercellular cytoplasm were significantly lower in the knockout mice than in the nonknockout mice (Fig. 4C–F). Subsequently, by determining the degree of mast cell activation and the partial source of IL-13, we found by WB that the

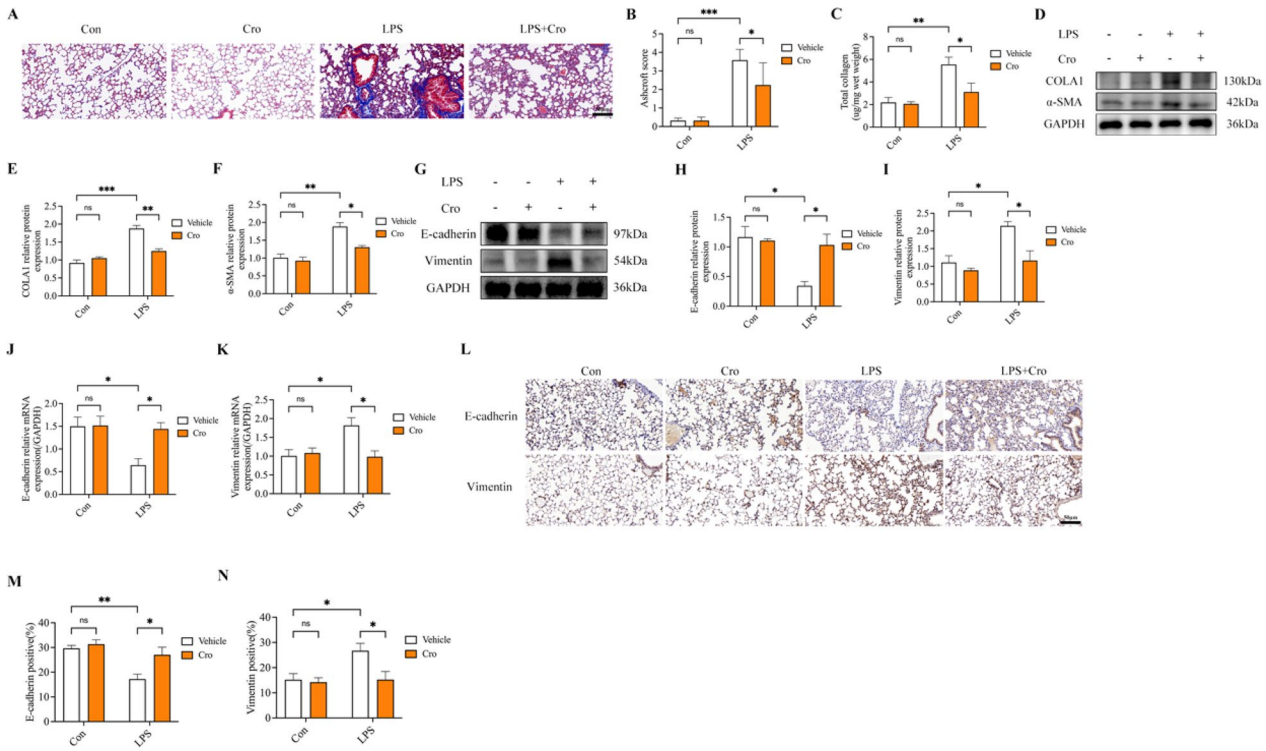

Fig. 3 Cromolyn sodium alleviates pulmonary fibrosis by inhibiting LPS-induced EMT. **A**, **B** A representative field of view of Masson staining and Ashcroft score after Cromolyn sodium intervention; scale bar: 50 μm, n = 5. **C** Interstitial hydroxyproline content of the lungs; n = 5. **D**–**F** Representative bands of collagen 1 and α-SMA proteins were analyzed, n = 3. **G**–**I** Representative bands of EMT-associated proteins were analyzed, n = 3. **J**, **K** mRNA expression levels of EMT-associated proteins, n = 6. **L**–**N** Representative field of view for EMT-associated protein immunohistochemistry and statistical analysis of the percentage of positive cells; scale bar: 50 μm, n = 5. *p < 0.05, **p < 0.01, ***p < 0.001

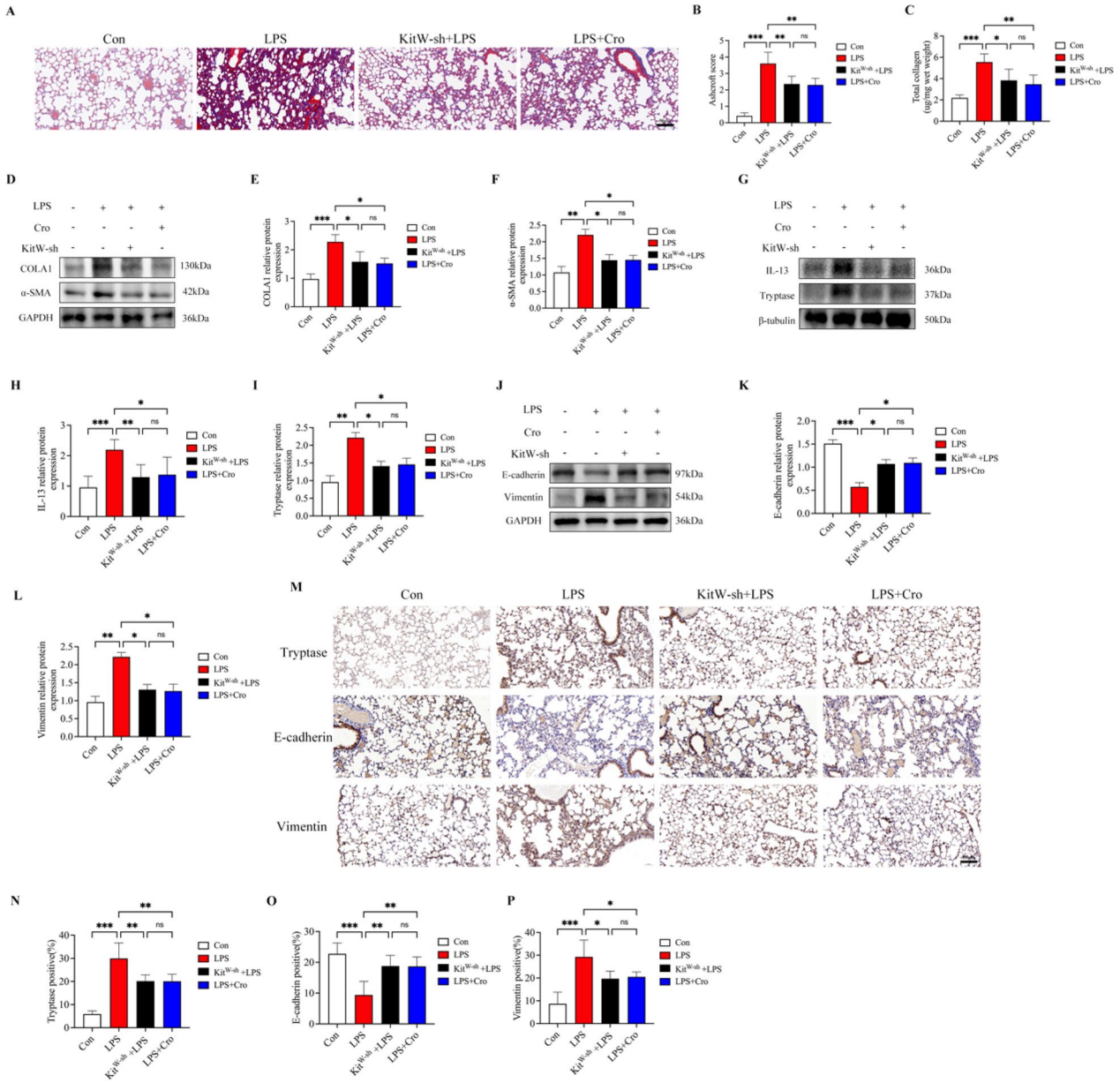

Fig. 4 Cromolyn sodium inhibits EMT and attenuates pulmonary fibrosis by reducing mast cell-derived IL-13. **A**, **B** Masson staining and Ashcroft scores of representative fields from mast cell knockout mice; scale bar: 50 μm; n = 5. **C** Hydroxyproline content of lung tissues in each group, n = 5. **D**–**F** Representative bands showing interstitial lung indexes in each group that were statistically analyzed; n = 3. **G**–**I** Representative bands of tryptase and IL-13 in each group were statistically analyzed, n = 3. **J**–**L** Representative bands of EMT-related indexes in each group were analyzed, n = 3. **M**–**Q** Representative field of view for EMT-associated protein and tryptase immunohistochemistry and statistical analysis of the percentage of positive cells; scale bar: 50 μm, n = 5. *p < 0.05, ***p < 0.001

activation level of tryptase in the lungs of knockout rats was slightly lower than that in the lungs of the intervention group and significantly lower than that in the lungs of the normal model group, and a similar trend was observed for IL-13 (Fig. 4G–I). The above results indicated that mast cell knockdown effectively inhibited mast cell activation in a mouse model of septic pulmonary fibrosis and effectively reduced the release of IL-13 from mast cells. Through previous studies, we found that Cromolyn sodium could inhibit EMT by suppressing mast cell activation, and this study further explored the effect of mast cell knockdown on EMT. Mast cell knockdown and treatment with Cromolyn sodium had similar inhibitory effects, and the levels of EMT-related genes

were significantly lower than those in the normal model group (Fig. 4J–L). In addition, the immunohistochemistry results were also consistent with the above results (Fig. 4M–P). The above results suggest that Cromolyn sodium can alleviate septic pulmonary fibrosis by reducing the release of IL-13 from mast cells and inhibiting EMT in animal experiments.

Cromolyn sodium inhibits EMT and attenuates pulmonary fibrosis by reducing mast cell-derived IL-13 release (in vitro)

In addition to in vivo experiments, we further verified the effect of Cromolyn sodium on mast cell activation and the release of IL-13 via in vitro experiments. First, to verify the effectiveness of Cromolyn sodium on the mouse mast cell line P815, we pretreated mast cells with 10 μg/ml Cromolyn for 30 min before induction with LPS, and cellular RNA, protein, and cell supernatant collection was performed 24 h after the intervention [30]. The WB results showed that Cromolyn sodium pretreatment significantly decreased P815 cell tryptase and IL-13 expression (Fig. 5A–C). In addition, we constructed an in vitro coculture system using a Transwell system for verification (Fig. 5D). Compared with alveolar epithelial cells without coculture, MLE-12 cells cocultured with mast cells exhibited increased levels of LPS-induced EMT, demonstrating that mast cells can promote the development of lung fibrosis by enhancing the level of EMT in alveolar epithelial cells (Fig. 5E–G). After that, we analyzed the levels of IL-13 in the supernatants of MLE-12

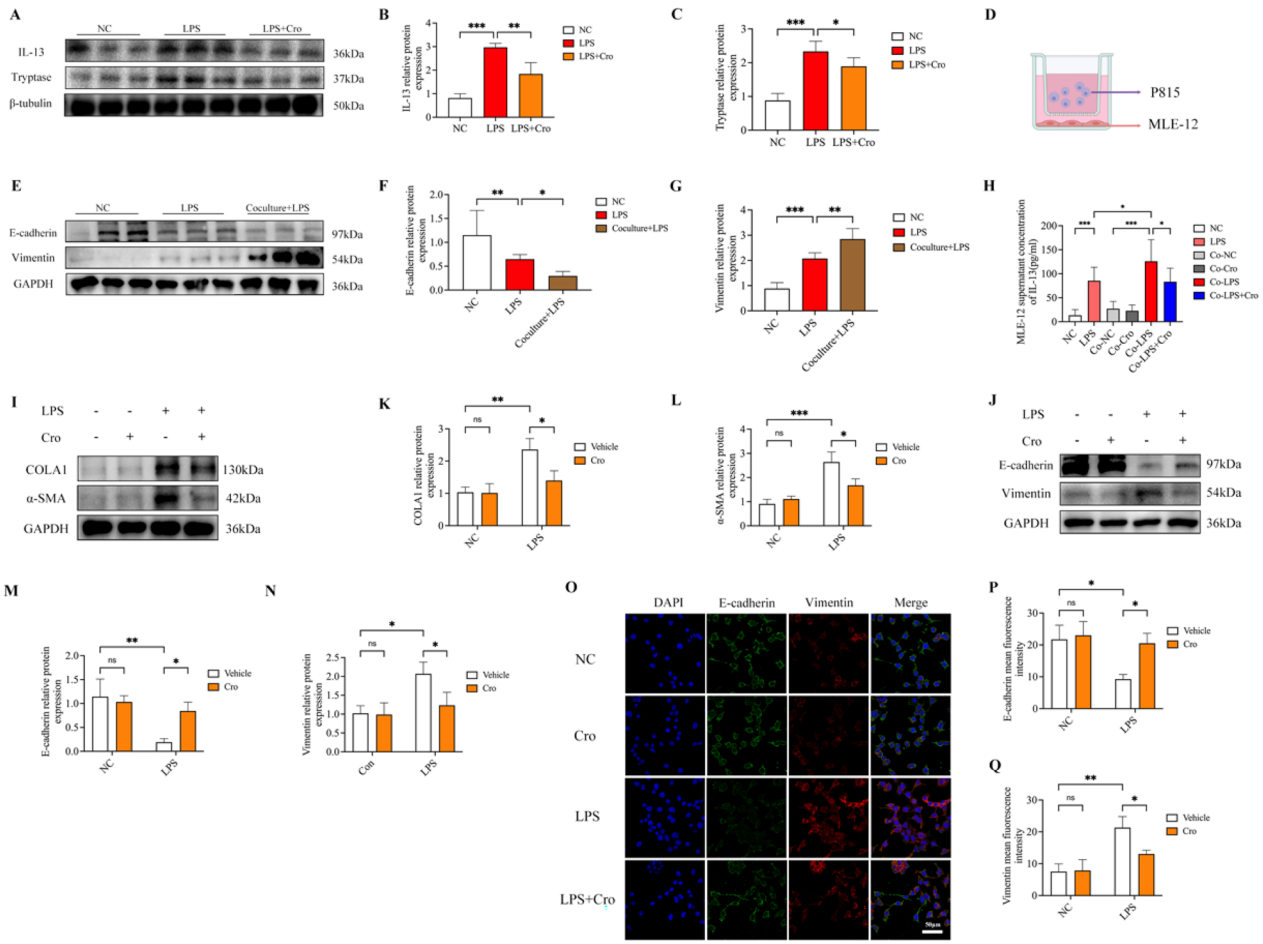

Fig. 5 Cromolyn sodium inhibits EMT and attenuates pulmonary fibrosis by reducing the release of mast cell-derived IL-13 (in vitro). **A**–**C** Effect of Cromolyn sodium intervention on the expression of tryptase and IL-13 in P815 cells and statistical analysis, n = 3. **D** Schematic diagram of coculture. **E**–**G** Effect of the coculture system on EMT in MLE-12 cells. **H** Differences in the levels of IL-13 in cell supernatants between the coculture groups and non-co-culture groups, n = 6. **I**–**L** Effect of Cromolyn sodium intervention on the interstitial quality indexes of the coculture groups, as determined by statistical analysis, n = 3. **J**–**N** Effects of Cromolyn sodium intervention on EMT indexes in the coculture groups and statistical analysis, n = 3. **O**–**Q** Statistical analysis of representative fields of view of immunofluorescence and the fluorescence intensity indicating the effects of Cromolyn sodium intervention on EMT indexes in MLE-12 cells; scale bar: 50 μm, n = 3. *p < 0.05, **p < 0.01, ****p < 0.001

cells. The results showed that the levels of IL-13 in the supernatants of MLE-12 cells in the coculture system were significantly greater than those in the supernatants of MLE-12 cells without coculture, and treatment with Cromolyn sodium reversed this effect. WB results showed that coculture significantly increased the expression of mesenchymal indicators in MLE-12 cells, while the level of E-cadherin was significantly decreased, and treatment with Cromolyn sodium alleviated the process of EMT (Fig. 5I–N). This finding was further supported by the immunofluorescence results (Fig. 5O–Q).

Mast cell-derived IL-13 regulates the LPS-induced EMT process (in vitro)

Although the above results demonstrated mast cell activation as well as a reduction in the level of IL-13 derived from mast cells after intervention, they do not directly indicate a direct role for mast cell-derived IL-13 in EMT. Therefore, we used small interfering RNA (siRNA) in an in vitro coculture system to knock down the expression of IL-13 in the mast cell line P815 to further verify the role of mast cell-derived IL-13. The results showed that after IL-13 knockdown, the level of IL-13 in the supernatant of MLE-12 cells was significantly decreased compared with that in the normal model group, while there was no statistically significant difference from that in the Cromolyn sodium intervention group (Fig. 6A). In addition, we also verified the relevant indexes of EMT, and the results showed that mast cell IL-13 knockdown significantly decreased the levels of IL-13 in the supernatants of alveolar epithelial cells and inhibited EMT (Fig. 6B–D). The immunofluorescence results further verified this finding (Fig. 6E–G).

MC-derived IL-13 regulates EMT through activation of the PI3K/AKT/mTOR pathway

EMT is currently believed to be regulated by several signaling pathways, one of which is the PI3K/AKT/mTOR pathway. It has also been shown that IL-13 can act as an important effector molecule to promote EMT. Therefore, we evaluated the differences in total PI3K, P-PI3K, total AKT, P-AKT, total mTOR and P-mTOR between in vivo and in vitro experiments. The results showed that in the animal experiments, total PI3K, total AKT, and total mTOR were not significantly changed in the lungs of any of the groups of mice, and phosphorylated proteins were significantly elevated in the normal model group, whereas Cromolyn sodium intervention significantly reversed the increase in phosphorylated proteins (Fig. 7A). Afterwards, we further verified this finding in an in vitro cellular assay (Fig. 7B). Subsequently, we verified the effect of mast cell knockdown on the PI3K/AKT/mTOR pathway, and the results showed that mast cell

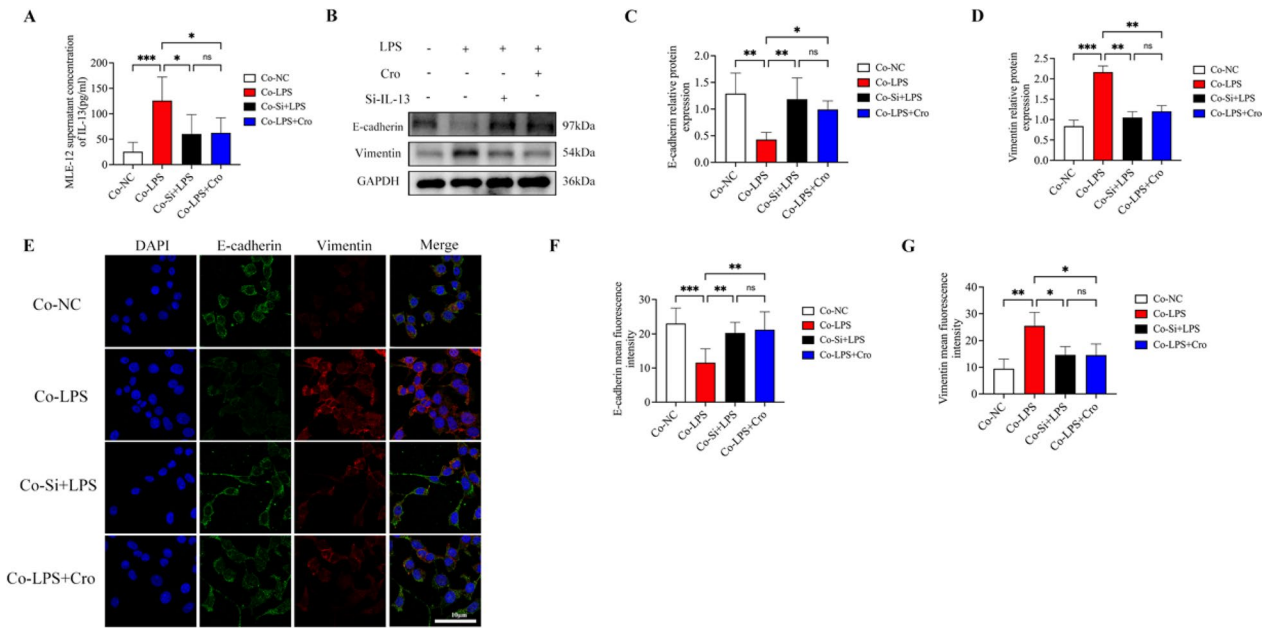

Fig. 6 Cromolyn sodium inhibits EMT and attenuates pulmonary fibrosis by reducing mast cell-derived IL-13. **A** The content of IL-13 in the supernatants of MLE-12 cells in each group of cocultured MLE-12 cells after knockdown of IL-13 in P815 cells, n = 6. **B**–**D** Representative protein bands of EMT-related indexes of MLE-12 cells in each group after knockdown of IL-13 in P815 cells and statistical analysis, n = 3. **E**–**G** Representative field of view and statistical analysis of fluorescence intensity for immunofluorescence of EMT-related indicators in MLE-12 cells; scale bar: 10 μm, n = 3. *p < 0.05, ***p < 0.01, ***p < 0.001

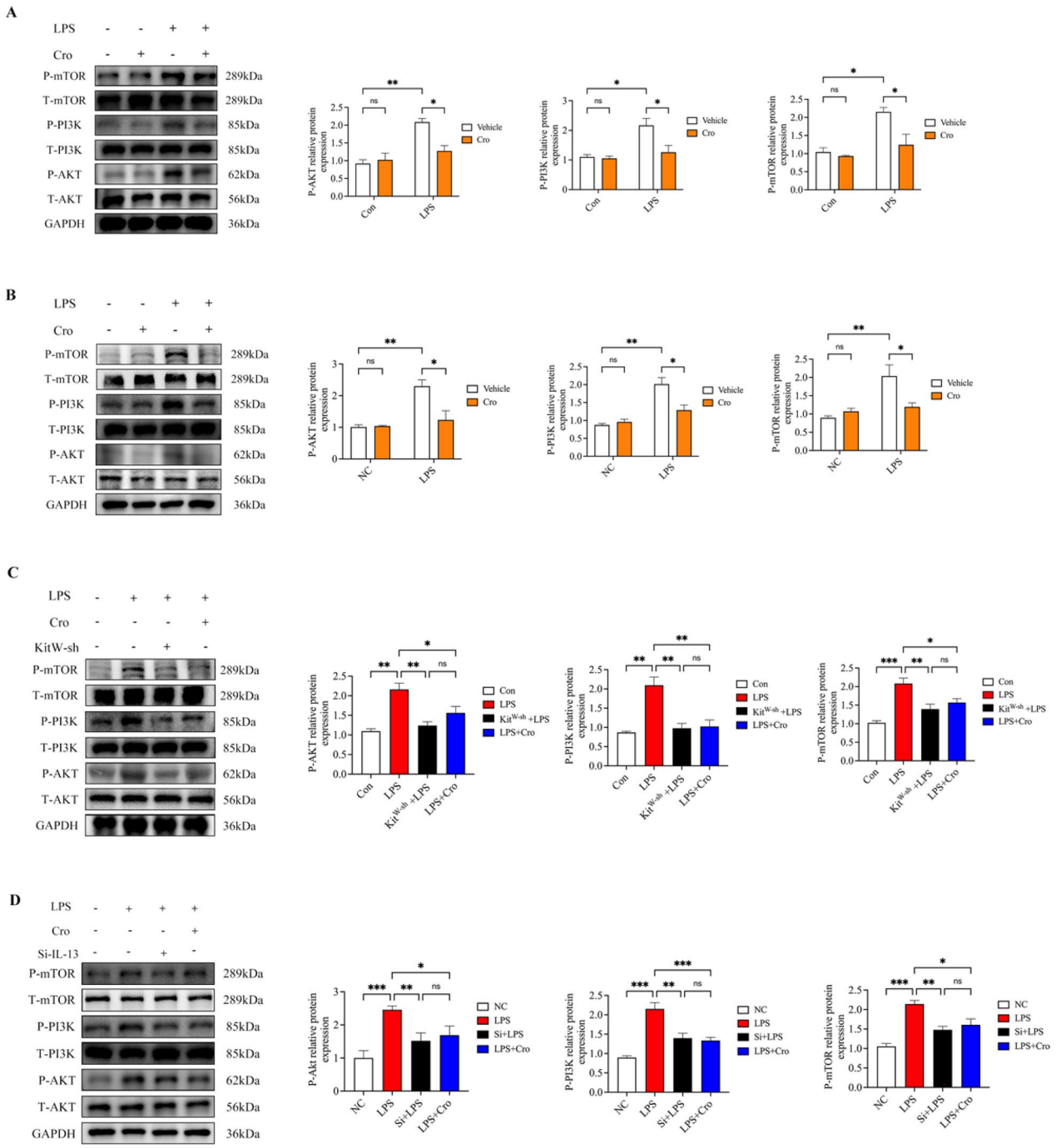

Fig. 7 Mast cell-derived IL-13 regulates EMT via activation of the PI3K/AKT/mTOR pathway. **A**, **B** Effects of Cromolyn sodium intervention on the PI3K/AKT/mTOR pathway in vivo and in vitro, n = 3. **C** Effects of mast cell knockdown on the PI3K/AKT/mTOR pathway. **D** Effects of IL-13 knockdown in P815 cells on the PI3K/AKT/mTOR pathway; n = 3. *p < 0.05, ***p < 0.01, ***p < 0.01, ***p < 0.001

knockdown also reversed the increase in phosphorylated proteins (Fig. 7C) and that the knockdown of mast cell IL-13 in vitro exerted the same effect (Fig. 7D). Interestingly, however, mast cell knockdown appeared to have a stronger inhibitory effect on the expression of phosphorylated proteins in animal experiments, but the exact reason for this effect remains to be further explored.

Discussion

It is well known that ARDS is a serious life-threatening clinical disease, pulmonary fibrosis associated with ARDS is a common complication, the occurrence of early pulmonary fibrosis suggests a high incidence of multiorgan failure and mortality, and there is no effective treatment [31, 32]. Infection is the most common cause of ARDS, and secondary pulmonary fibrosis has become an important cause of poor prognosis. Even if patients survive, pulmonary fibrosis can seriously affect quality of life [33, 34]. Therefore, exploring the mechanisms of ARDS-associated pulmonary fibrosis and possible interventions is clinically important for reducing ARDS mortality. Dysregulation of EMT is a potential causative agent of pulmonary fibrosis disease, and thus, reversing the EMT process may be a potential target for improving pulmonary fibrosis.

Animal models of various diseases are designed to create a 'translation bridge' between the patient and the laboratory: hypotheses developed during human studies can be directly confirmed or refuted in experiments on laboratory animals, and the results of in vitro experiments can be successfully verified in vivo. In humans, lung inflammation begins before the onset of clinical signs of ALI/ARDS and peaks within the first three days of disease onset [35], accompanied by destruction of lung endothelial and epithelial cells, alveolar and interstitial oedema and disruption of gas exchange [36]. Therefore, animal models of acute lung injury should be able to reproduce the inflammatory response and disruption of the epithelial/endothelial barrier of lung tissue. Furthermore, a more complex aspect of modelling human ALI on laboratory animals (e.g., mice and rats) is that patients with ALI may have a primary disease that results in ALI (e.g., sepsis) and/or receive some therapeutic and supportive treatment (e.g., mechanical lung ventilation) [37]. Therefore, none of the available animal models of ALI reflect all the characteristics of human ALI. However, depending on the aim of the study, a thorough selection of murine models could help to answer urgent questions about the molecular mechanisms underlying the development and regulation of ALI. LPS is a major component of the outer membrane of Gram-negative bacteria that triggers local and systemic inflammatory responses. It is closely associated with lung injury and is frequently used to induce lung inflammation in in vivo models [38–40]. LPS acts as a potent activator of the innate immune response through a TLR4-dependent pathway, making this model a prime model for studying inflammatory responses similar to that during bacterial infections, which are induced by intraperitoneal injection of LPS leading to septic systemic infection and ultimately the acute phase of ALI/ARDS, the histological features and the inflammatory response to bacterial infection are more closely aligned to the clinical presentation, making the results more convincing. In contrast, bleomycin, which is used by the majority of the population, is an antitumor antibiotic with little association with the stimulus that triggers the development of fibrosis in humans. In this study, we used an intraperitoneal injection of LPS to establish a mouse model of sepsis-associated pulmonary fibrosis. This model was more closely related to the real pathogenesis than the bleomycin-induced pulmonary fibrosis model. The results showed that the expression of mast cells and IL-13 was significantly increased in the fibrotic lungs of the model mice. Moreover, changes in E-cadherin, Vimentin and other related proteins also indicated the occurrence of EMT. Knockdown of the mast cell stabilizer Cromolyn sodium as well as mast cells reduced the expression of lung fibrosis-related proteins in the lung tissues of LPS-induced mice by inhibiting the production of IL-13 as well as EMT and improving the symptoms of fibrosis. In addition, a coculture system of mast cells and alveolar epithelial cells was constructed in this study, and by knocking down IL-13-expressing genes in mast cells, it was further demonstrated that mast cells may promote the development of EMT through the production of IL-13, which contributes to the development of pulmonary fibrosis in sepsis. These processes are dependent on the PI3K/AKT/mTOR signaling pathway in alveolar epithelial cells (Fig. 8).

Mast cells are abundant in healthy airways and lung parenchyma and are increased in the fibrotic areas of the alveolar parenchyma in patients with pulmonary fibrosis, including infants with idiopathic pulmonary fibrosis, chronic hypersensitivity pneumonitis, sarcoidosis, silicosis, and bronchopulmonary dysplasia [41–43]. Increased numbers of mast cells have also been found in bronchoalveolar lavage fluid from patients with various interstitial lung diseases. In several studies, the number of mast cells in the fibrotic lung parenchyma or bronchoalveolar lavage fluid was positively correlated with the severity of fibrosis and negatively correlated with lung function. Therefore, the number of mast cells in alveolar lavage fluid may have prognostic significance [44]. Morphologically, mast cells in the fibrotic parenchyma of patients with IPF and other interstitial lung diseases usually exhibit a reduced number of granules and disorganized granule content, suggesting that some mast cells undergo degranulation. There is also evidence of increased release of trypsin-like enzymes in the tissue, demonstrating that mast cells are being activated, but the exact mechanism is unclear. It has recently been demonstrated that Mast-Cell Expressed Membrane Protein-1 (MCEMP1) may play a role in the pathogenesis of IPF by regulating the migration and transformation of monocytes to alveolar

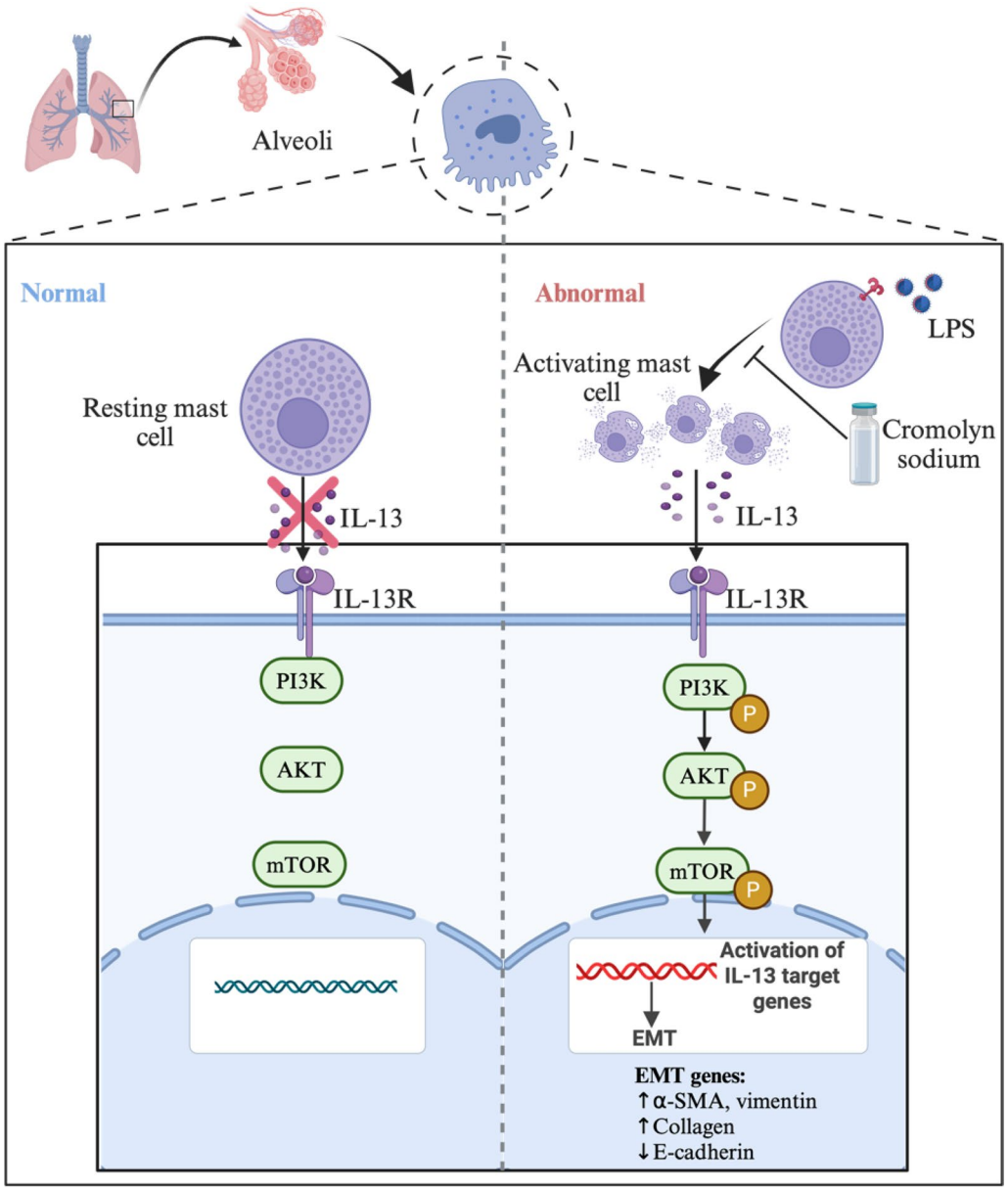

Fig. 8 Working model

macrophages of monocyte origin. This suggests that mast cells may also be involved in the process of pulmonary fibrosis by interacting with other cells, which provides a further avenue for research and a referable direction [45]. In the present study, we also found increased release of trypsin-like enzymes within lung tissue in the fibrotic lung tissue of septic mice induced by intraperitoneal injection of LPS. However, whether mast cell activation is beneficial or detrimental to pulmonary fibrosis has different results in different animal models. In a bleomycin-induced lung fibrosis rat model, mast cell knockout rats had a greater degree of lung fibrosis than normal control rats, whereas both groups of mice exhibited approximately the same degree of lung fibrosis [46]. Remarkably, the lungs of bleomycin mast cell knockout mice had higher levels of hydroxyproline than did those of normal mice, suggesting that mast cells may actually play a protective role. In contrast, in a model of lung fibrosis induced by allergic respiratory inflammation, compared with normal mice, mast cell knockout mice exhibited reduced fibrosis, suggesting that mast cells may play a deleterious role in lung fibrosis [47–50]. In the present

study, we found that septic lung fibrosis was attenuated by Cromolyn sodium in mice with mast cell inhibition or systemic knockout compared with that in normal mice, suggesting that activated mast cells may play a deleterious role in sepsis-associated acute lung injury and lung fibrosis.

Although the initiating factors and specific role of inflammation in pulmonary fibrosis remain unelucidated, there is evidence that events such as sustained damage to the alveolar epithelium and capillary endothelium, chronic injury leading to dysregulation of repair, proliferation and mesenchymal transition of type II alveolar epithelium, and generation of fibroblastic foci contribute to the development of pulmonary fibrosis. These events are driven by several profibrotic mediators. Epithelial injury stimulates the release of several mediators, including TGF-β1, which is a key upstream profibrotic growth factor that drives IPF. In addition, a number of profibrotic factors are released from other cells, including PDGF, FGF-2, IL-4, and IL-13, which can contribute to the development of pulmonary fibrosis by promoting collagen synthesis and EMT [51–54]. In the present study, we found that the expression of IL-13 was significantly elevated in the lungs of mice with septic pulmonary fibrosis, suggesting that it plays a role in the LPS-induced septic pulmonary fibrosis model. We therefore hypothesized that intraperitoneally injected LPS activates mast cells and promotes their release of the pro-fibrotic cytokine IL-13 by binding to the TLR4 receptor on mast cells, which promotes the progression of pulmonary fibrosis by promoting EMT in alveolar epithelial cells. This was confirmed by our findings that significant EMT occurred in the lung tissues of mice after intraperitoneal injection of LPS, whereas a significant decrease in IL-13 and pulmonary fibrosis was observed after treatment with Cromolyn sodium or mast cell knockdown, and at the same time, the level of EMT was also alleviated. In the in vitro experiments, we constructed a system of cocultures of mast cell P815 cells and the alveolar epithelial cell line MLE-12 to further verify that IL-13 partly originated from mast cells and mainly acted by promoting EMT. We induced EMT in MLE-12 cells with LPS, whereas the levels of IL-13 in the cell supernatants were significantly greater and the degree of EMT was greater after coculture. In contrast, the degree of EMT in MLE-12 cells was significantly reduced after treatment with Cromolyn sodium or after knockdown of IL-13 in mast cells. These results also validated our hypothesis that, at least in vitro, Cromolyn sodium could alleviate pulmonary fibrosis by inhibiting the release of IL-13 from mast cells. However, unlike the expected complete reversal of pulmonary fibrosis, both in vivo and in vitro, Cromolyn sodium and mast cell knockdown could only partially ameliorate LPS-induced pulmonary fibrosis but not completely ameliorate it, suggesting that the involvement of mast cell release of IL-13 in the progression of pulmonary fibrosis is only a part of the many pathogenic mechanisms of septic pulmonary fibrosis and that additional mechanisms remain to be further investigated.

The PI3K/AKT/mTOR signaling pathway plays an important role in regulating cell proliferation, survival and angiogenesis [55]. Activation of the PI3K/AKT pathway by various stimuli initiates a series of signaling events that promote cell survival, proliferation and metabolism. AKT is the central node of this pathway, which phosphorylates and activates a number of downstream targets, including mTOR. mTOR pathway, especially mTOR complex 1 (mTORC1), is an important regulator of cell growth and metabolism, affecting protein synthesis. mTOR is a key regulator of cell growth and metabolism, affecting protein synthesis autophagy and lipid metabolism. Notably, the PI3K/AKT/mTOR pathway was significantly upregulated in PF [56]. For example, LPS induces fibroblast proliferation and collagen synthesis through this pathway [57]. LPS promotes aerobic glycolysis in lung fibroblasts through the PI3K/AKT/mTOR pathway, leading to increased collagen production. This metabolic shift, often referred to as the Warburg effect, supports the energy and biosynthetic requirements of proliferating fibroblasts and myofibroblasts in fibrotic tissues. Inhibitors targeting the PI3K/AKT/mTOR pathway have shown promise in preclinical PF models. For example, clonidine ethanolamine salts alleviate PF by modulating the PI3K/mTORC1 pathway and reducing fibroblast proliferation and extracellular matrix deposition. Similarly, pharmacological inhibition of mTOR using drugs such as rapamycin attenuates fibroblast activation and collagen synthesis, highlighting the therapeutic potential of targeting this pathway [58]. In addition, previous studies have focused on fibroblasts and, or myofibroblasts, rather than alveolar epithelial cells. Thus, the different models as well as the different targets of action aroused our interest in selecting this pathway of mTOR. Previous studies have shown that the PI3K/AKT/mTOR pathway mediates the process of EMT [59, 60]. Pretreatment with the PI3K inhibitor LY294002 and the mTOR inhibitor rapamycin inhibited this process [55, 61]. In addition, activation of the PI3K/AKT/mTOR signaling pathway is involved in the LPS-induced EMT process [62]. In contrast, in a study by Baek et al., ginkgolic acid C15:1 (GA C15:1) inhibited lung cancer invasion, metastasis, and EMT by inhibiting the PI3K/AKT/mTOR signaling pathway, whereas the activation of PI3K/AKT increased the expression of matrix metalloproteinase-9, degraded E-cadherin, and promoted cell invasion and migration [63]. A study by Park,G. B, Activation of PI3K induced

the EMT process in LPS-stimulated SKOV-3 cells in a Syk/Src-dependent manner [64]. This evidence prompted us to explore whether the PI3K/AKT/mTOR signaling pathway is involved in the process of mast cell-mediated LPS-induced EMT. The results showed that the PI3K/AKT/mTOR signaling pathway was activated in the LPS-induced sepsis lung fibrosis model, whereas cromoglycate intervention or mast cell knockdown significantly inhibited the LPS-induced phosphorylation of PI3K/AKT/mTOR. In vitro coculture experiments revealed that knockdown of IL-13 in mast cells also significantly inhibited PI3K/AKT/mTOR phosphorylation, but in the present study, the pathway was superficial, and no additional experiments were performed to demonstrate the roles of the three proteins in conjunction with each other. Further studies are not possible through the use of activators or inhibitors, which will be further investigated in the future.

Interestingly, unlike what we had previously envisioned, Cromolyn sodium intervention appeared to have a better therapeutic effect than complete mast cell knockdown. This may be related to the role of Cromolyn sodium itself, a mast cell stabilizer with anti-inflammatory activity that has neuroprotective and antioxidant effects in addition to its ability to prevent mast cells from triggering an immune response, and oxidative stress is one of the important mechanisms of alveolar epithelial injury. In recent articles, mast cells have typically been discussed in the context of disease, including cardiovascular disease [65], cancer [66], airway disease [67], and roles in viral, bacterial, and fungal infections [68–70]. Importantly, however, they also play a role in the homeostasis of the inner environment, in the initiation of acute inflammation, and in defense against dangers, whether external (venoms, pathogens, etc.) or internal (cell damage, fungal infections, etc.). On the one hand, mast cells are able to secrete a large number of inflammatory mediators, including histamine, interleukins, leukotrienes, TNF-α, prostaglandins, proteases, TGF-β, CCL5, etc., which in turn activate a multitude of cell-surface receptors and promote inflammation through the corresponding signaling pathways. Mast cells, on the other hand, play a role in pathogen recognition and clearance. In the context of LPS infection, this function is mainly associated with Toll-like receptors (TLR) and complement receptors expressed on the surface of mast cells, which respond to invading pathogens in a specific manner by releasing appropriate anti-inflammatory inflammatory mediators. Also, the increased vascular permeability initiated by mast cells contributes to bacterial clearance, permitting the recruitment of natural killer cells (NK cells), eosinophils, and neutrophils to help kill bacteria. And in viral infections, mast cells participate in the clearance of viral pathogens by recruiting interferon-producing T cells. Mast cells also produce an anti-parasitic environment and increase vascular permeability and smooth muscle contraction, which helps eliminate parasites. In addition, mast cells are involved in the regulation of a wide range of cell types, including T cells, B cells, dendritic cells, endothelial cells, and epithelial cells, so it plays a role in many physiological functions, including wound healing, bone formation, angiogenesis, and mineral homeostasis. In contrast, the complete mast cell knockout in the article may lead to a complete loss of the anti-inflammatory effects of mast cells, which ultimately produces the discrepancy between the therapeutic effects of sodium cromoglycate intervention and complete mast cell knockout. Therefore, complete mast cell inhibition may also not be the best option for the treatment of septic pulmonary fibrosis, and inhibiting its proinflammatory effects while exerting its anti-inflammatory effects may be a better direction for research.

In addition, this study has several limitations. First, we did not prove the mast cell origin of IL-13 by immunofluorescence colocalization, immunohistochemistry, or tracer techniques but rather reversed the partial origin of IL-13 by changes in IL-13 expression before and after intervention and knockdown. In addition, we did not use inhibitors or neutralizing antibodies against IL-13 in animal experiments to confirm its ability to promote EMT. Systemic rather than specific knockdown of mast cells also failed to exclude effects on other organs. Activation of mast cells leads to the release of a variety of mediators that can act on cells or related substrates in different organs and systems to produce clinically relevant symptoms. Actions on the nervous system may result in anxiety, reduced concentration or depression. Effects on the cardiovascular system may result in hypertension, syncope or tachycardia. Effects on the digestive system may result in abdominal pain, reflux or nausea and vomiting. But mast cells don't always play a harmful role, and some studies have shown that in murine models of myocardial infarction and myocarditis, mast cells have been shown to improve rather than worsen cardiac contractility. In the nervous system, mast cells also play a bidirectional role. On the one hand, central mast cells regulate neurogenesis, promote hippocampal development, and participate in neuroprotection. On the other hand, overactivation of mast cells can also lead to disruption of the blood–brain barrier, neuroinflammation, and neuropathic pain. Therefore, systemic knockdown of mast cells may have effects on multiple systems, but systemic knockdown is difficult to achieve in humans, and the effects of systemic knockdown on individual systems are more often observed in animal models. In

the first generation of knockout models, it was caused by various mutations in Kit (i.e., the SCF receptor). Since SCF is an important growth factor for MCs, Kit defects resulted in essentially complete knockout in mast cells. However, many other cell types also express KIT, so it has been a challenge to determine that the consequence of Kit knockdown is indeed an effect on MCs rather than an off-target effect on other cells [71, 72]. In this article, we used the first-generation knockout model, the most obvious manifestation of which is the change in its hair color, which may be related to the lack of melatonin secretion after mast cell knockout, which has been shown to have antidepressant and anxiolytic effects. To address the above issues, new Kit-independent mast cell knockout models have been developed, including mice that cause mast cell knockout by Cre recombinase expression under the control of a mast cell-specific promoter, but such mice have the obvious disadvantage of causing a decrease in the number of basophils, and their effects on various systems need to be further investigated [73, 74]. In conclusion, although we conclude that Cromolyn sodium may be a potential drug for the treatment of septic pulmonary fibrosis, the ameliorative effect of Cromolyn sodium on septic pulmonary fibrosis still needs to be validated by further clinical evidence and clinically relevant studies.

For future studies, it is important to evaluate the specific knockdown of mast cells in models of septic pulmonary fibrosis. In addition, considering that IL-13 is associated with pulmonary fibrosis, specific knockdown of IL-13 in mast cells would be very helpful for subsequent studies. In addition, sepsis-induced pulmonary fibrosis is a long-term process, and the activation pattern of mast cells may be different at different stages. Treatment at different times may have different therapeutic effects, so it may be therapeutically important to explore the mechanism of mast cell involvement in sepsis-induced pulmonary fibrosis at different stages.

Acknowledgements
Not applicable.

Author contributions
TC, ZH, YH and XJJ: designed the study, analyzed the data and wrote the manuscript. TC, ZH and XX: acquired and analyzed data. TC, ZH and XQF: performed experiments. LQY and ZZX: analyzed the data and helped to write the paper. YH and XJJ: provided the financial support for this work. All authors read and approved the final manuscript.

Funding
This study was supported by the Provincial Key R&D Program (Social Development) of Science And Technology Department Of Jiangsu Province (No. BE2021748) and the Wuxi Municipal Commission Fund of Health Planning (No. M202345).

Availability of data and materials
The mast cell knockout mice used during the current study are available from the corresponding author on reasonable request.

Declarations

Ethics approval and consent to participate
This study was approved by the Institutional Animal Care and Use Committee (IACUC) of Nanjing Medical University (No. 2207016).

Consent for publication
Not applicable.

Competing interests
The authors declare no competing interests.

Received: 13 July 2024 Accepted: 17 November 2024
Published online: 06 January 2025

References

1. Gorman EA, O'Kane CM, McAuley DF. Acute respiratory distress syndrome in adults: diagnosis, outcomes, long-term sequelae, and management. Lancet. 2022;400(10358):1157–70.
2. Butt Y, Kurdowska A, Allen TC. Acute lung injury: a clinical and molecular review. Arch Pathol Lab Med. 2016;140(4):345–50.
3. Thannickal VJ, Toews GB, White ES, Lynch JP 3rd, Martinez FJ. Mechanisms of pulmonary fibrosis. Annu Rev Med. 2004;55:395–417.
4. Cottin V, Wollin L, Fischer A, Quaresma M, Stowasser S, Harari S. Fibrosing interstitial lung diseases: knowns and unknowns. Eur Respir Rev. 2019;28(151):180100.
5. Thannickal VJ, Zhou Y, Gaggar A, Duncan SR. Fibrosis: ultimate and proximate causes. J Clin Invest. 2014;124(11):4673–7.
6. Marino KV, Cagnoni AJ, Croci DO, Rabinovich GA. Targeting galectin-driven regulatory circuits in cancer and fibrosis. Nat Rev Drug Discov. 2023;22(4):295–316.
7. Wynn TA, Ramalingam TR. Mechanisms of fibrosis: therapeutic translation for fibrotic disease. Nat Med. 2012;18(7):1028–40.
8. Thiery JP, Acloque H, Huang RY, Nieto MA. Epithelial-mesenchymal transitions in development and disease. Cell. 2009;139(5):871–90.
9. Kimura K, Orita T, Liu Y, Yang Y, Tokuda K, Kurakazu T, et al. Attenuation of EMT in RPE cells and subretinal fibrosis by an RAR-gamma agonist. J Mol Med (Berl). 2015;93(7):749–58.
10. Cao L, Xiao M, Wan Y, Zhang C, Gao X, Chen X, et al. Epidemiology and mortality of sepsis in intensive care units in prefecture-level cities in Sichuan, China: a prospective multicenter study. Med Sci Monit. 2021;27:e932227.
11. Wilcock A, Bahri R, Bulfone-Paus S, Arkwright PD. Mast cell disorders: from infancy to maturity. Allergy. 2019;74(1):53–63.
12. Wernersson S, Pejler G. Mast cell secretory granules: armed for battle. Nat Rev Immunol. 2014;14(7):478–94.
13. Hershey GK. IL-13 receptors and signaling pathways: an evolving web. J Allergy Clin Immunol. 2003;111(4):677–90.
14. Melo-Cardenas J, Bezavada L, Crawford JC, Gurbuxani S, Cotton A, Kang G, et al. IL-13/IL-4 signaling contributes to fibrotic progression of the myeloproliferative neoplasms. Blood. 2022;140(26):2805–17.
15. Roeb E. Interleukin-13 (IL-13)-a pleiotropic cytokine involved in wound healing and fibrosis. Int J Mol Sci. 2023;24(16):12884.
16. Lurje I, Gaisa NT, Weiskirchen R, Tacke F. Mechanisms of organ fibrosis: emerging concepts and implications for novel treatment strategies. Mol Aspects Med. 2023;92:101191.
17. Zhao J, Jiang T, Li P, Dai L, Shi G, Jing X, et al. Tissue factor promotes airway pathological features through epithelial-mesenchymal transition of bronchial epithelial cells in mice with house dust mite-induced asthma. Int Immunopharmacol. 2021;97:107690.
18. Katoh M, Nakagama H. FGF receptors: cancer biology and therapeutics. Med Res Rev. 2014;34(2):280–300.
19. Chi M, Liu J, Mei C, Shi Y, Liu N, Jiang X, et al. TEAD4 functions as a prognostic biomarker and triggers EMT via PI3K/AKT pathway in bladder cancer. J Exp Clin Cancer Res. 2022;41(1):175.

20. Yu M, Qi B, Xiaoxiang W, Xu J, Liu X. Baicalein increases cisplatin sensitivity of A549 lung adenocarcinoma cells via PI3K/Akt/NF-kappaB pathway. Biomed Pharmacother. 2017;90:677–85.
21. Cong LH, Li T, Wang H, Wu YN, Wang SP, Zhao YY, et al. IL-17A-producing T cells exacerbate fine particulate matter-induced lung inflammation and fibrosis by inhibiting PI3K/Akt/mTOR-mediated autophagy. J Cell Mol Med. 2020;24(15):8532–44.
22. Yuan R, Fan Q, Liang X, Han S, He J, Wang QQ, et al. Cucurbitacin B inhibits TGF-beta1-induced epithelial-mesenchymal transition (EMT) in NSCLC through regulating ROS and PI3K/Akt/mTOR pathways. Chin Med. 2022;17(1):24.
23. Huang CY, Deng JS, Huang WC, Jiang WP, Huang GJ. Attenuation of lipopolysaccharide-induced acute lung injury by hispolon in mice, through regulating the TLR4/PI3K/Akt/mTOR and Keap1/Nrf2/HO-1 pathways, and suppressing oxidative stress-mediated ER stress-induced apoptosis and autophagy. Nutrients. 2020;12(6):1742.
24. Yang Y, Sun Y, Xu J, Bao K, Luo M, Liu X, et al. Erratum to "epithelial cells attenuate toll-like receptor-mediated inflammatory responses in monocyte-derived macrophage-like cells to mycobacterium tuberculosis by modulating the PI3K/Akt/mTOR signaling pathway." Mediators Inflamm. 2021;2021:3710790.
25. Kim SY, Jeong E, Joung SM, Lee JY. PI3K/Akt contributes to increased expression of Toll-like receptor 4 in macrophages exposed to hypoxic stress. Biochem Biophys Res Commun. 2012;419(3):466–71.
26. Blackwell TS, Christman JW. The role of nuclear factor-kappa B in cytokine gene regulation. Am J Respir Cell Mol Biol. 1997;17(1):3–9.
27. Chandra SM, Razavi H, Kim J, Agrawal R, Kundu RK, de Jesus PV, et al. Disruption of the apelin-APJ system worsens hypoxia-induced pulmonary hypertension. Arterioscler Thromb Vasc Biol. 2011;31(4):814–20.
28. Xiao K, He W, Guan W, Hou F, Yan P, Xu J, et al. Mesenchymal stem cells reverse EMT process through blocking the activation of NF-kappaB and Hedgehog pathways in LPS-induced acute lung injury. Cell Death Dis. 2020;11(10):863.
29. Roviezzo F, Sorrentino R, Iacono VM, Brancaleone V, Terlizzi M, Riemma MA, et al. Disodium cromoglycate inhibits asthma-like features induced by sphingosine-1-phosphate. Pharmacol Res. 2016;113(Pt A):626–35.
30. Yue J, Tan Y, Huan R, Guo J, Yang S, Deng M, et al. Mast cell activation mediates blood-brain barrier impairment and cognitive dysfunction in septic mice in a histamine-dependent pathway. Front Immunol. 2023;14:1090288.
31. Meyer NJ, Gattinoni L, Calfee CS. Acute respiratory distress syndrome. Lancet. 2021;398(10300):622–37.
32. Bos LDJ, Ware LB. Acute respiratory distress syndrome: causes, pathophysiology, and phenotypes. Lancet. 2022;400(10358):1145–56.
33. Fang XZ, Li M, Wang YX, Zhang P, Sun MM, Xu JX, et al. Mechanosensitive ion channel Piezo1 mediates mechanical ventilation-exacerbated ARDS-associated pulmonary fibrosis. J Adv Res. 2023;53:175–86.
34. Meduri GU, Eltorky MA. Understanding ARDS-associated fibroproliferation. Intensive Care Med. 2015;41(3):517–20.
35. Park WY, Goodman RB, Steinberg KP, Ruzinski JT, Radella F 2nd, Park DR, et al. Cytokine balance in the lungs of patients with acute respiratory distress syndrome. Am J Respir Crit Care Med. 2001;164:1896–903.
36. Berthiaume Y, Matthay MA. Alveolar edema fluid clearance and acute lung injury. Respir Physiol Neurobiol. 2007;159(3):350–9.
37. Mikacenic C, Moore R, Dmyterko V, West TE, Altemeier WA, Liles WC, et al. Neutrophil extracellular traps (NETs) are increased in the alveolar spaces of patients with ventilator-associated pneumonia. Crit Care. 2018;22(1):358.
38. Jiang K, Guo S, Yang C, Yang J, Chen Y, Shaukat A, et al. Barbaloin protects against lipopolysaccharide (LPS)-induced acute lung injury by inhibiting the ROS-mediated PI3K/AKT/NF-kappaB pathway. Int Immunopharmacol. 2018;64:140–50.
39. Soromou LW, Chen N, Jiang L, Huo M, Wei M, Chu X, et al. Astragalin attenuates lipopolysaccharide-induced inflammatory responses by down-regulating NF-kappaB signaling pathway. Biochem Biophys Res Commun. 2012;419(2):256–61.
40. Zhang B, Liu ZY, Li YY, Luo Y, Liu ML, Dong HY, et al. Antiinflammatory effects of matrine in LPS-induced acute lung injury in mice. Eur J Pharm Sci. 2011;44(5):573–9.
41. Inoue Y, King TE Jr, Tinkle SS, Dockstader K, Newman LS. Human mast cell basic fibroblast growth factor in pulmonary fibrotic disorders. Am J Pathol. 1996;149(6):2037–54.
42. Groot Kormelink T, Pardo A, Knipping K, Buendia-Roldan I, Garcia-de-Alba C, Blokhuis BR, et al. Immunoglobulin free light chains are increased in hypersensitivity pneumonitis and idiopathic pulmonary fibrosis. PLoS ONE. 2011;6(9):e25392.
43. Wygrecka M, Dahal BK, Kosanovic D, Petersen F, Taborski B, von Gerlach S, et al. Mast cells and fibroblasts work in concert to aggravate pulmonary fibrosis: role of transmembrane SCF and the PAR-2/PKC-alpha/Raf-1/p44/42 signaling pathway. Am J Pathol. 2013;182(6):2094–108.
44. Andersson CK, Andersson-Sjoland A, Mori M, Hallgren O, Pardo A, Eriksson L, et al. Activated MCTC mast cells infiltrate diseased lung areas in cystic fibrosis and idiopathic pulmonary fibrosis. Respir Res. 2011;12(1):139.
45. Perrot CY, Karampitsakos T, Unterman A, Adams T, Marlin K, Arsenault A, et al. Mast-cell expressed membrane protein-1 is expressed in classical monocytes and alveolar macrophages in idiopathic pulmonary fibrosis and regulates cell chemotaxis, adhesion, and migration in a TGFbeta-dependent manner. Am J Physiol Cell Physiol. 2024;326(3):C964–77.
46. Mori H, Kawada K, Zhang P, Uesugi Y, Sakamoto O, Koda A. Bleomycin-induced pulmonary fibrosis in genetically mast cell-deficient WBB6F1-W/Wv mice and mechanism of the suppressive effect of tranilast, an antiallergic drug inhibiting mediator release from mast cells, on fibrosis. Int Arch Allergy Appl Immunol. 1991;95(2–3):195–201.
47. Masuda T, Tanaka H, Komai M, Nagao K, Ishizaki M, Kajiwara D, et al. Mast cells play a partial role in allergen-induced subepithelial fibrosis in a murine model of allergic asthma. Clin Exp Allergy. 2003;33(5):705–13.
48. Yu M, Tsai M, Tam SY, Jones C, Zehnder J, Galli SJ. Mast cells can promote the development of multiple features of chronic asthma in mice. J Clin Invest. 2006;116(6):1633–41.
49. Reber LL, Daubeuf F, Pejler G, Abrink M, Frossard N. Mast cells contribute to bleomycin-induced lung inflammation and injury in mice through a chymase/mast cell protease 4-dependent mechanism. J Immunol. 2014;192(4):1847–54.
50. Veerappan A, O'Connor NJ, Brazin J, Reid AC, Jung A, McGee D, et al. Mast cells: a pivotal role in pulmonary fibrosis. DNA Cell Biol. 2013;32(4):206–18.
51. Xu YD, Hua J, Mui A, O'Connor R, Grotendorst G, Khalil N. Release of biologically active TGF-beta1 by alveolar epithelial cells results in pulmonary fibrosis. Am J Physiol Lung Cell Mol Physiol. 2003;285(3):L527–39.
52. Tarantal AF, Chen H, Shi TT, Lu CH, Fang AB, Buckley S, et al. Overexpression of transforming growth factor-beta1 in fetal monkey lung results in prenatal pulmonary fibrosis. Eur Respir J. 2010;36(4):907–14.
53. Gharaee-Kermani M, Hu B, Phan SH, Gyetko MR. Recent advances in molecular targets and treatment of idiopathic pulmonary fibrosis: focus on TGFbeta signaling and the myofibroblast. Curr Med Chem. 2009;16(11):1400–17.
54. Henderson NC, Rieder F, Wynn TA. Fibrosis: from mechanisms to medicines. Nature. 2020;587(7835):555–66.
55. Engelman JA. Targeting PI3K signalling in cancer: opportunities, challenges and limitations. Nat Rev Cancer. 2009;9(8):550–62.
56. Glaviano A, Foo ASC, Lam HY, Yap KCH, Jacot W, Jones RH, et al. PI3K/AKT/mTOR signaling transduction pathway and targeted therapies in cancer. Mol Cancer. 2023;22(1):138.
57. Hu X, Xu Q, Wan H, Hu Y, Xing S, Yang H, et al. PI3K-Akt-mTOR/PFKFB3 pathway mediated lung fibroblast aerobic glycolysis and collagen synthesis in lipopolysaccharide-induced pulmonary fibrosis. Lab Invest. 2020;100(6):801–11.
58. Pei X, Zheng F, Li Y, Lin Z, Han X, Feng Y, et al. Niclosamide ethanolamine salt alleviates idiopathic pulmonary fibrosis by modulating the PI3K-mTORC1 pathway. Cells. 2022;11(3):346.
59. Xu W, Yang Z, Lu N. A new role for the PI3K/Akt signaling pathway in the epithelial-mesenchymal transition. Cell Adh Migr. 2015;9(4):317–24.
60. Karimi Roshan M, Soltani A, Soleimani A, Rezaie Kahkhaie K, Afshari AR, Soukhtanloo M. Role of AKT and mTOR signaling pathways in the induction of epithelial-mesenchymal transition (EMT) process. Biochimie. 2019;165:229–34.
61. Jiao D, Wang J, Lu W, Tang X, Chen J, Mou H, et al. Curcumin inhibited HGF-induced EMT and angiogenesis through regulating c-Met dependent PI3K/Akt/mTOR signaling pathways in lung cancer. Mol Ther Oncolytics. 2016;3:16018.

62. Jiang M, Zhou LY, Xu N, An Q. Hydroxysafflor yellow A inhibited lipopolysaccharide-induced non-small cell lung cancer cell proliferation, migration, and invasion by suppressing the PI3K/AKT/mTOR and ERK/MAPK signaling pathways. Thorac Cancer. 2019;10(6):1319–33.
63. Baek SH, Ko JH, Lee JH, Kim C, Lee H, Nam D, et al. Ginkgolic acid inhibits invasion and migration and TGF-beta-induced EMT of lung cancer cells through PI3K/Akt/mTOR inactivation. J Cell Physiol. 2017;232(2):346–54.
64. Park GB, Chung YH, Kim D. Induction of galectin-1 by TLR-dependent PI3K activation enhances epithelial-mesenchymal transition of metastatic ovarian cancer cells. Oncol Rep. 2017;37(5):3137–45.
65. Varricchi G, Marone G, Kovanen PT. Cardiac mast cells: underappreciated immune cells in cardiovascular homeostasis and disease. Trends Immunol. 2020;41(8):734–46.
66. Varricchi G, de Paulis A, Marone G, Galli SJ. Future needs in mast cell biology. Int J Mol Sci. 2019;20(18):4397.
67. Virk H, Arthur G, Bradding P. Mast cells and their activation in lung disease. Transl Res. 2016;174:60–76.
68. Piliponsky AM, Acharya M, Shubin NJ. Mast cells in viral, bacterial, and fungal infection immunity. Int J Mol Sci. 2019;20(12):2851.
69. Jiao Q, Luo Y, Scheffel J, Zhao Z, Maurer M. The complex role of mast cells in fungal infections. Exp Dermatol. 2019;28(7):749–55.
70. Rathore AP, St John AL. Protective and pathogenic roles for mast cells during viral infections. Curr Opin Immunol. 2020;66:74–81.
71. Rodewald HR, Feyerabend TB. Widespread immunological functions of mast cells: fact or fiction? Immunity. 2012;37(1):13–24.
72. Reber LL, Marichal T, Galli SJ. New models for analyzing mast cell functions in vivo. Trends Immunol. 2012;33(12):613–25.
73. Dudeck A, Dudeck J, Scholten J, Petzold A, Surianarayanan S, Kohler A, et al. Mast cells are key promoters of contact allergy that mediate the adjuvant effects of haptens. Immunity. 2011;34(6):973–84.
74. Feyerabend TB, Weiser A, Tietz A, Stassen M, Harris N, Kopf M, et al. Cre-mediated cell ablation contests mast cell contribution in models of antibody- and T cell-mediated autoimmunity. Immunity. 2011;35(5):832–44.

Publisher's Note